KERNFORSCHUNGSZENTRUM KARLSRUHE

März 1966

KFK 413

Institut für Neutronenphysik und Reaktortechnik

Two-Detector Crosscorrelation Experiments in the Fast-Thermal Argonaut Reactor STARK

W. Seifritz, D. Stegemann, W. Väth

GESELLSCHAFT FÜR KERNFORSCHUNG M. B. H.

KARLSRUHE

KERNFORSCHUNGSZENTRUM KARLSRUHE

März 1966 KFK 413

Institut für Neutronenphysik und Reaktortechnik

TWO-DETECTOR CROSSCORRELATION EXPERIMENTS IN THE FAST-THERMAL ARGONAUT REACTOR STARK+

W.Seifritz, D.Stegemann, W.Väth

Paper presented at the International Symposium on Neutron Noise, Waves, and Pulse Propagation held at Gainesville, Florida, February 14 - 16, 1966.

+Work performed within the association in the field of fast reactors between the European Atomic Energy Community and Gesellschaft für Kernforschung mbH, Karlsruhe

Gesellschaft für Kernforschung m.b.H. Karlsruhe

ABSTRACT

Autopower and crosspower spectral density measurements have been performed in the externally unperturbed Fast-Thermal Argonaut Reactor STARK, using the frequency analysis of noise technique. Theoretical considerations showed the advantage of two-detector crosscorrelation experiments over single-detector autocorrelation experiments, because the contribution of uncorrelated noise is eliminated in the output-signal. This was verified experimentally. The advantage of the crosscorrelation method is particularly important, if only low detector efficiency is available, as is the case, for instance, in fast reactors. In view of this, a detailed experimental program has been performed to show the extent to which the autopower and crosspower technique is applicable.

Different detectors have been placed into the fast core region and into the thermal core region of STARK. Because detector efficiency is mainly responsible for the ratio of correlated to uncorrelated reactor noise, the efficiency was changed during the program. In order to obtain reliable results from the data for the prompt neutron decay constant, reactivity, and absolute reactor power it was found that for the single-detector experiment the ratio of correlated to uncorrelated noise must be at least 2, whereas for the two-detector crosscorrelation experiment reliable results have been found with values of the ratio down to 0.1. The necessary time for sampling and analysis increases with decreasing values of the ratio. This has been theoretically confirmed by calculation of the relative standard deviation in crosspower spectral density experiments. The calculated deviations have also been checked experimentally.

An optical correlation demonstrator is described which can be used to show the degree of correlation in a quick and simple manner.

INTRODUCTION

The analysis of noise phenomena in reactors is part of a larger reactor physics program in Karlsruhe which is carried out for the development of fast breeder power reactors. In the first phase of the noise program particular stress is given to zero power neutronic noise analysis in order to determine the prompt neutron decay constants in fast-thermal and fast zero power reactor assemblies like STARK[1] and SNEAK[2]. As is well known, there is still a remarkable discrepancy between the caluclated and measured neutron lifetime in dilute fast systems. Because of the importance of this integral parameter - sensitive in particular to spectral effects, which affect again the breeding gain, the Doppler coefficient etc. - a precise determination is a necessity. Furthermore, we feel zero power noise analysis is interesting for the study of fast-thermal coupled systems as well as for the determination of reactivity values and absolute reactor power.

In context with the program the question arose, which method is best suited to solve the problems. To find the answer the first step was a thorough theoretical analysis accompanied by the investigation of several experimental techniques. The theoretical effort finally resulted in a basic theoretical model[3] from which known and new techniques could be derived. The combined experimental effort resulted in a comparison[4] of three noise analysis methods together with the pulsed neutron source technique. Although the results agreed quite well, the answer to the question put up was not straight forward. It rather turned out that the conclusions from theory and experiments were more of specific nature. The application of the ROSSI-α-technique, for example, has advantages for the investigation of uranium-fueled fast-thermal coupled systems, because well separated decay constants can be directly determined by the experiment. The method seems to be disadvantageous for measurements at the delayed critical state in large plutonium-fueled fast assemblies. In this respect, on the contrary, the power spectral density technique offers great advantages, which will be discussed in detail below. To come back to the question under consideration our answer at the present state is: There exists no unique noise analysis technique, which covers the whole range of possible applications with optimum efficiency. In order to find the best experimental procedure the

specific features of the problem encountered have to be analysed. This analysis is possible, because the theoretical investigations made by the different authors in the noise field give already a good insight into the problems.

During the course of the theoretical noise analysis [3] it has been found already early in 1964 that in crosspower spectral density measurements with two detectors the contribution of uncorrelated noise to the correlator output signal must disappear. This was proved experimentally, and earlier results were shown in the comparative study [4]. This fact has been investigated since that time more deeply by a systematic comparison of autopower and crosspower spectral density experiments.

The theoretical procedure to find the equations for autocorrelation and crosscorrelation experiments will not be repeated here. In the point reactor model approximation and for high frequencies (neglecting delayed neutrons) we found for the two cases:

(a) Single-detector autocorrelation experiment

$$\frac{\overline{r^2}(\omega, \Delta\omega)}{\Gamma(\omega, \Delta\omega)} = W F \overline{q}^2 \left[R + \frac{W \varkappa_2 k^2}{\ell^2(\alpha^2 + \omega^2)} \right], \qquad (1)$$

(b) Two-detector crosscorrelation experiment

$$\frac{\overline{r_1 r_2}(\omega, \Delta\omega)}{\Gamma(\omega, \Delta\omega)} = \overline{q_1}\,\overline{q_2} F \frac{W_1 W_2 \varkappa_2 k^2}{\ell^2(\alpha^2 + \omega^2)} . \qquad (2)$$

The symbols used are:

r_n = actual output on line n (n = 1, 2)

$\Gamma(\omega, \Delta\omega) = \mathrm{Re} \int_0^\infty \frac{d\omega'}{\pi} B_1(\omega') B_2(-\omega')$ = characteristic parameter of bandfilters

ω = angular frequency = $2\pi f$

$\Delta\omega$ = frequency interval to be analysed

$B_n(\omega)$ = frequency characteristic of filter n

$\overline{q_n}$ = average charge released per detected neutron

W_n = efficiency of detector n (in counts per fission in the system)

F = fission rate in the system

$R = \frac{\overline{q^2}}{\overline{q}^2} \geq 1$, factor accounting for statistical fluctuations of the ionisation phenomena

$\varkappa_2 = \frac{\overline{\nu(\nu-1)}}{\overline{\nu}^2}$; ν = number of neutrons per fission

k = effective multiplication constant

ℓ = prompt neutron lifetime

$\alpha = \frac{1 - k\,(1 - ß)}{\ell}$ = decay constant of prompt neutron flux

ß = effective fraction of delayed neutrons.

All measurements referred to in this paper were performed at the delayed critical state. Subcritical measurements were not of interest in this connection. In the critical case is $\alpha = \alpha_c = \frac{ß}{\ell}$ and k = 1, and equations (1) and (2) reduce to

$$\frac{\overline{r^2}(\omega, \Delta\omega)}{\Gamma(\omega, \Delta\omega)} = W F \overline{q}^2 R + \frac{W^2 F \overline{q}^2 \varkappa_2}{ß^2 + \ell^2 \omega^2} \qquad (3)$$

and

$$\frac{\overline{r_1 r_2}(\omega, \Delta\omega)}{\Gamma(\omega, \Delta\omega)} = \overline{q_1}\,\overline{q_2} F \frac{W_1 W_2 \varkappa_2}{ß^2 + \ell^2 \omega^2} \,. \qquad (4)$$

The measured quantities on the left hand side of (3) and (4) give the autopower spectral density and the crosspower spectral density respectively. The first term on the right hand side of (3) is the contribution from uncorrelated reactor noise to the autopower spectral density in the single-detector experiment, whereas the second term gives the correlated noise contribution.

The specific feature of the crosscorrelation experiment, namely the absence of a contribution from uncorrelated events to the correlator output signal, is clearly shown by (4).

To find the ratio of correlated to uncorrelated detector events eq.(3) will be discussed. Using $\alpha_c = \frac{\beta}{\ell}$ the correlated contribution in the autocorrelation experiment can be written as

$$A = \frac{W^2 F \overline{q}^2 \varkappa_2}{\beta^2} \cdot \frac{1}{1 + (\omega/\alpha_c)^2} \quad . \tag{3a}$$

The uncorrelated contribution is frequency independent and follows from the first term of (3) as

$$U = W F \overline{q}^2 R \quad . \tag{3b}$$

The ratio of correlated to uncorrelated contribution is given by

$$Q(\omega) = \frac{A}{U} = \frac{\varkappa_2}{\beta^2 R} W \frac{1}{1 + (\omega/\alpha_c)^2} \quad . \tag{5}$$

For crosspower spectral density measurements the correlated part C is directly given by (4). For estimation of errors in crosspower spectral density experiments - see eq.(10) - it is necessary to know the following ratios:

$$Q_1(\omega) = \frac{C}{U_1} = \frac{\varkappa_2}{\beta^2 R} W_2 \frac{1}{1 + (\omega/\alpha_c)^2} \tag{5a}$$

and

$$Q_2(\omega) = \frac{C}{U_2} = \frac{\varkappa_2}{\beta^2 R} W_1 \frac{1}{1 + (\omega/\alpha_c)^2} \quad . \tag{5b}$$

The ratios have their largest values if $\omega^2 \ll \alpha_c^2$, that is for low frequencies in the order of 1 cps. Therefore, in this frequency range the quotient in the denominator can be neglected and the maximum value is

$$Q_{1,2\,max} = \frac{\varkappa_2}{\beta^2 R} \cdot W_{2,1} \quad . \tag{6}$$

It has been assumed $\overline{q_1} = \overline{q_2}$ and $R_1 = R_2$.

Insertion of (6) into (5) yields

$$Q_n(\omega) = \frac{Q_{n\,max}}{1 + (\omega/\alpha_c)^2} \quad . \tag{7}$$

The maximum ratio depends besides constants only on detector efficiency. It should be noted, that due to the lower value of ß in a fast plutonium-fueled reactor, the same Q_{max} can be achieved with a lower detector efficiency than in a thermal uranium-fueled reactor. To be independent of those effects the ratio Q_{max} has been chosen as a criterion for comparing auto- and crosspower spectral density measurements. Additional reasons are that the ratio can be easily derived from autocorrelation experiments and the factor R is difficult to determine experimentally. The explicit knowledge of R, ß, and γ_2 would be necessary if the detector efficiency W had been chosen as criterion rather than the ratio Q_{max}.

The aim of the experimental program was (a) to show the advantage of crosscorrelation over autocorrelation for decreasing values of Q_{max} and (b) to investigate the practical lower limit of Q_{max}, so that still reliable results can be found in reasonable times for data analysis. Therefore, the value of Q_{max} was changed systematically, and at each point auto- and crosspower spectral density measurements were conducted.

EXPERIMENTAL SETUP

All experiments were performed in loading no.2 of the coupled fast-thermal zero power reactor STARK[1] at 10 watts. A schematic cross section is shown in FIG.1. Basically the reactor consists of a cylindrical fast core (37 cm average diameter, 61 cm height), which is surrounded by an annular Argonaut type thermal driver zone and a large graphite reflector. As shown in FIG.1 the fast core is an array of 37 vertical stainless steel matrix tubes filled with the core material to be investigated. In this loading the enrichment in the fast zone was 7% ^{235}U (45.25 kg). The fast core is enclosed in a natural uranium buffer zone of 5 cm average thickness to absorb thermal neutrons incident from the outside. The thermal zone contained 332 Argonaut fuel plates (^{235}U-content 6.92 kg) arranged in 24 groups with a plate spacing of 6.2 mm. The moderator was light water at 80°C.

According to fission chamber traverses the power fractions are about 9% in the fast zone, 11% in the natural uranium buffer zone and 80% in the thermal region. Although the thermal zone is still the leading part of the reactor, power spectral density measurements were also performed in the fast section at the positions indicated. Here, ^{3}He-filled counting tubes have been used in the current mode of operation. For auto- and cross-power spectral density measurements in the thermal region two ^{10}B-loaded γ-compensated ion chambers were located at different positions in the reflector (see FIG.1).

The equipment used is shown in the block diagram of FIG.2. The output signals from the amplifiers were stored on a multichannel magnetic tape recorder. This is advantageous because the tape speed-up technique can be used so that the time for analysing the signals, particularly at low frequencies, is reduced considerably.

A short comment should be made to the application of the ^{3}He counting tubes. Before starting the actual measurements the ^{3}He-filled proportional counters have been tested at their usual operating voltage of about 4.5 kv. After this test the voltage has been lowered to about 200 volts and the mean current has been observed as a function of applied voltage. Almost no change of the mean current was found in the range of 200 to ca. 1000 volts. Therefore, the operating voltage for the current mode has been set at 380 volts.

The frequency response of the analysing equipment had to be chosen according to the break frequency of the zero power transfer function under investigation. The response is determined by the RC-value of detector capacity and amplifier input impedance, the amplifier response itself, the frequency range of the magnetic tape recorder, and by the response of the bandfilters and multiplier circuits. The input resistor of the amplifiers used was about 10 megohm and the capacities of detectors, cables etc. were about 125 u uF (^{3}He counting tubes) and 500 u uF (^{10}B-chambers), so that the upper break frequency was 132 cps and 33 cps, respectively. All other parts of the equipment had upper frequencies exceeding the frequency range to be analysed. The amplifier response is flat and has its upper break frequency (3 db point) at 100 kcps. The magnetic tape recorder goes up to

1.25 kcps in the FM mode of operation (3 3/4 ips). The frequency range of the band pass filters reaches from 0.2 to 20 kcps. The relative bandwidth $\Delta f/f$ was always chosen to be 0.95. The multiplier and integrator circuits have upper frequency limits of 2.5 kcps and their dynamic range is sufficient. The frequency response of the equipment was checked by "white noise" measurements in a thermal column so that the correction factors for the measured power spectral densities were confirmed experimentally. In fast zero power systems where the frequency range must extend to about 10 kcps the RC-value of the detector amplifier system causes problems if the input resistance R cannot be lowered because of current or amplifier design reasons. A possibility to overcome this difficulty is the use of pulse detectors connected to fast counting rate circuits[5].

EXPERIMENTS AND RESULTS

The experimental runs performed are listed in TAB.1. Run no.1-3 were planned for two reasons. The first one was to investigate whether ^{3}He-filled proportional counting tubes could be used in the current mode of operation for power spectral density measurements. This is especially interesting for experiments in fast systems, for ^{3}He has a relatively large reaction cross section in the neutron energy range present, and it allows furthermore high filling gas pressures so that the efficiencies in fast systems are better than those of ^{10}B and fission detectors. The second reason was to find out whether the crosspower spectral density versus frequency curve measured in the fast core differs from that one measured in the thermal region. The results of run no.1-3 are plotted in FIG.3. The curves demonstrate the applicability of ^{3}He counting tubes for power spectral density measurements. Although equal tubes were used in both positions, the curve for pos.19 shows a lower efficiency than that for pos.30. This is due to the flux profile in the fast zone with its minimum in the core center. From the 3 curves already here the advantage of crosscorrelation over autocorrelation is visible. The crosspower spectral density versus frequency curve in the fast core does not differ from those measured in the thermal zone as can be seen from a comparison of FIG.3 - 6. Therefore, also the values for α_c, listed in TAB.1, agree within the error limits. This result was expected because, as mentioned above, only 9% of the total power is generated in the fast section. This will be different in future loadings of STARK where the enrichment in the fast core is to be increased.

Run No. 4 - 10 were planned to study the dependence of auto- and crosspower measurements on the ratio Q_{max} - given by (6) - and to find the lowest practical value for the crosscorrelation technique. The procedure was to change the ratio Q_{max} by withdrawing the chambers step by step from the inner to the outer region of the reflector. In run no.4 and 5 autopower spectral density measurements were performed for each chamber at the positions B_1 and K_1, indicated in FIG.1. From these the ratio Q_{max} could be obtained dividing the constant value of the autopower spectral density around 1 cps (uncorrelated plus correlated contribution) by the constant value at high frequencies (uncorrelated contribution). This yields using (3) and (5) for the case $\ell^2\omega^2 \ll \beta^2$

$$\left(W F \bar{q}^2 R + \frac{W^2 F \bar{q}^2 \chi_2}{\beta^2} \right) \frac{1}{W F \bar{q}^2 R} = 1 + \frac{\chi_2}{\beta^2 R} W = 1 + Q_{max} . \qquad (8)$$

The value for the ratio Q_{max} determined in this manner is listed in TAB.1. For the equal chambers in positions B_1 and K_1 the ratio is larger for K_1 because it is more adjacent to the thermal core. The crosspower spectral density curve measured with the two chambers in positions B_1 and K_1 is also given in FIG.4. The α_c-values derived by least squares fitting technique are listed in TAB.1. For run no.7 and 8 the chamber in position B_1 was removed to position B_2 so that the mean current was approximately 25% of that in position B_1. The chamber in K_1 was withdrawn to a point where the mean current was equal to that of the chamber in B_2. This point is marked K_2. Because the chamber efficiencies were equal now in B_2 and K_2 only one autopower spectral density measurement was performed to find Q_{max}. This and the corresponding crosspower spectral density measurement between K_2 and B_2 are shown in FIG.5. The decrease of Q_{max} to about 0.5 affects the autocorrelation experiment remarkably. For run no.9 and 10 the chambers were further withdrawn to positions K_3 and B_3 where their mean current was equal again but the magnitude only about 20% of that in K_2 and B_2, respectively. The autopower spectral density curve in FIG.6 is almost flat and the ratio Q_{max} drops to ca. 0.1. In this case, in which no information can be gained from autocorrelation experiments, the two-detector crosscorrelation method yields still reliable results. This fact is clearly demonstrated by the crosspower curve in FIG.6. It should be pointed out,

however, that the time required for analysis is increased if Q_{max} is decreased. Quantitative considerations to this problem are given in the next section. It may be mentioned for completeness that equivalent values of autopower and crosspower spectral densities have not been corrected for differences in absolute gain factor.

From the experimental results it can be concluded that for single-detector autocorrelation measurements a ratio Q_{max} of at least 2 is necessary to obtain the prompt neutron decay constant properly. Two-detector crosscorrelation measurements can be carried out to values as low as $Q_{max} = 0.1$, which has been found a practical limit. Referring back to (6) this means a reduction factor of ca. 20 in detector efficiency.

The significance of this result for fast reactor systems may be illustrated by a simple example. If fission chambers are used in the experiments the efficiency is roughly given by the ratio of fissionable material in the chamber to fissionable material in the reactor. For $Q_{max}=0.1$ the minimum efficiency can be calculated from (6) using $\beta = 3.3 \cdot 10^{-3}$ and $\chi_2 = 0.8$, R = 1.2, typical figures for fast systems and detectors. This results in $W_{min} = 1.6 \cdot 10^{-6}$. The largest commercially available chambers have layers of about 2 gr fissionable material, so that the critical mass of the reactor to be investigated could go up to about 1260 kg. The application of the single-detector method would be limited already at 63 kg.

The behaviour of the two-detector crosscorrelation technique is also favorable for thermal systems. Although the situation concerning efficient detectors is much better, crosspower spectral density experiments can be performed to more subcritical states, which is interesting for calibration of safety rods and other reactivity measurements.

The absolute reactor power was also derived from the measured power spectral densities and the mean chamber currents. The values obtained did not differ more than 10% from those found by foil activations and calibrated fission chamber traverses.

ERROR ESTIMATION FOR CROSSPOWER SPECTRAL DENSITY MEASUREMENTS

The suppression of the uncorrelated noise contribution in the mean product $\overline{r_1 r_2}(\omega, \Delta\omega)$ is due to the multiplication process in the crosscorrelator. It must not be forgotten that the uncorrelated contribution is still present in the filter output signals $r_1(t)$ and $r_2(t)$. So, the desired random noise input to the correlator, which is the correlated part, is modified by additional uncorrelated random noise disturbances. The error estimation for this special case has been extensively treated by BENDAT [6]. The results of his theoretical considerations are - to a certain extent - applicable to our problem. It is assumed that the noise contributions to the correlator input signals are mutually independent and have characteristics of normal random noise. These facts are approximately fulfilled in the experiments if only moderate detector efficiencies are used. The theory includes the use of bandfilters preceding the correlator. BENDAT [6] obtained for the variance σ^2_{xy} in crosspower spectral density measurements the equation

$$\sigma^2_{xy} = \frac{S^2\left[\kappa + (N_1/S) + (N_2/S) + (N_1/S)\cdot(N_2/S)\right]}{bT} \quad \text{, for } bT \geq 10^4 \text{ ,} \qquad (9)$$

S, N_1, and N_2 represent the input mean square (power) values (in our case C, U_1, U_2), and

κ = constant, $1 < \kappa < 2$

b = $\pi \Delta f = \pi \cdot$ bandwidth

T = sampling time.

With the terminology used so far and by introduction of the relative standard deviation, ε_{CPSD}, in crosspower spectral density measurements (9) leads to

$$\varepsilon_{CPSD} = \frac{\sigma_{xy}}{C} \cong \left[\frac{\kappa + (Q_1)^{-1} + (Q_2)^{-1} + (Q_1 Q_2)^{-1}}{\pi \Delta f\, T}\right]^{\frac{1}{2}} \text{ ,} \qquad (10)$$

for $\pi \Delta f\, T \geq 10^4$ and $1 < \kappa < 2$.

The crosspower spectral density is given by (4) and the ratios Q_n by (5a) and (5b), respectively.

Decreasing ratios Q_n enlarge the numerator of (10). For constant relative standard deviations ε_{CPSD} the denominator has to be increased accordingly, which means, the use of longer sampling times T if the bandwidth Δf is kept constant. Usually also Δf is increased at higher frequencies so that not all the compensation for lower Q_n-values has to be borne by T.

The reliability of (10) was checked experimentally in two ways: (a) The denominator of (10) was kept constant and only the numerator was changed by variation of the Q_{max}-values. This was performed by measurements in positions K_1, K_2, K_3, and B_1, B_2, B_3, respectively. The center frequency of the bandfilter (f = 1 cps), the filter bandwidth (Δf = 0.95 cps) and the sampling time (T = 10240 sec) were kept constant in this set of runs. TAB.2 contains the comparison of the calculated relative standard deviations, ε_{CPSD}(Calc.), and the deviations found experimentally, ε_{CPSD}(Exp.). To find the experimental values a set of runs was repeated about 10 times and from the resulting error probability distribution the variance (i.e. the mean square variation about the mean value) was determined. (b) The numerator as well as the denominator was changed in this case by variation of the center frequency f and the bandwidth Δf according to Δf = 0.95 f. B_2 and K_2 were chosen as detector positions and remained unchanged in this series of runs. The Q_n-values depend strongly on frequency, as can be seen from (5). Experimental relative standard deviations were determined as in (a). In TAB.2 calculated and measured deviations ε_{CPSD} are compared at different frequencies.

The results of the two series of runs (a) and (b) show that eq.(10) allows a reasonable statistical error estimation for the points on the crosspower spectral density curve. Because of this a better estimation of accuracy for the prompt neutron decay constant itself is possible. On the other hand, (10) is advantageous to estimate sampling times if a certain accuracy is required. For optimum conditions of an experiment also the bandwidth chosen should be equal to the frequency resolution necessary but not less.

The relative standard deviation ε_{APSD} for an autocorrelation experiment follows from (9) for $N_1 = N_2 = 0$,

$$\varepsilon_{APSD} = \frac{\sigma}{S} = \left[\frac{\kappa}{\pi \Delta f\ T}\right]^{\frac{1}{2}} , \tag{11}$$

which is known from literature[5] .

Now S represents autopower spectral density (3) and consists of a correlated part, A, and an uncorrelated part, U, (3a, 3b).

The correlated contribution can be calculated from

$$A = S - U . \tag{12}$$

Both S and U are measured with an accuracy given by ε_{APSD}, which is assumed to be independent of frequency in the following derivation.

The relative standard deviation ε_A for the correlated part in autocorrelation is found by the GAUSSIAN error propagation law to be

$$\varepsilon_A = \left[\frac{\kappa (1 + 2Q^{-1} + 2Q^{-2})}{\pi \Delta f\ T}\right]^{\frac{1}{2}} . \tag{13}$$

Only for values of the ratio $Q > 10$ this is approximated by

$$\varepsilon_A = \left[\frac{\kappa}{\pi \Delta f\ T}\right]^{\frac{1}{2}} . \tag{14}$$

OPTICAL DEMONSTRATION OF CORRELATION

The registration of uncorrelated and correlated events from neutron chains by the detectors must express itself in the behaviour of the output signals under investigation. In a two-detector crosscorrelation experiment where mutually independent events are detected no similarity of the two output signals is expected. Such a case has been traced in FIG.7, where the filter output signals as function of time are shown for channel 1 and 2. The center frequency was f = 1 cps and the bandwidth Δf = 0.95 cps.

The signals do not show common characteristics. This must be different if correlated events due to branching processes within reaction chains are present. If observation periods are long enough - which is the case for a center frequency of 1 cps - the appearance of correlated events within the chains is fully contained in the signals. Therefore, the correlation between the two signals must express itself in similar amplitudes as well as in zero crossings at equivalent points on the time axis. The similarity of the two filter output signals should be the more distinct the higher the contribution of correlated noise. This behaviour is clearly visible in FIG.8. The filter output signals (f = 1cps; Δf = 0.95cps) are shown for the chambers in position B_1 and K_1. A special case in this context is the single-detector autocorrelation experiment which can be treated formally as crosscorrelation experiment with two identical signals.

The correlation of the signals in the two-detector experiment is optically demonstrated more clearly if the one filter output signal drives the x-axis of an oscilloscope and the other the y-axis, and if the resulting traces on the screen are photographed for a sufficient time to receive geometric planes as shown in FIG.9a to 9e. For fully uncorrelated signals the curves of constant light intensity are circles (FIG.9a). The other extreme case, the autocorrelation experiment with two identical signals, gives a straight line inclined (45° angle) to the x- and y-axes (FIG.9e). The ratios Q have been increased by variation of the center frequency from higher to lower values in FIG.9b to 9d. The amount of correlation in the signals is, therefore, directly optically visible.

Under the appropriate assumption that the amplitude distribution of both the correlated and uncorrelated part in the signals x and y is nearly GAUSSIAN, the curves of constant light intensity are ellipses. For the case where the ellipses major axes incline 45° to the x- and y-axes the following relation is obtained [7]:

$$\frac{a^2}{b^2} = \frac{L + 1}{L - 1}, \qquad (15)$$

where a and b are the major and minor ellipses semi axes, and

$$L = \sqrt{(1 + \frac{1}{Q_1^{2/3}})(1 + \frac{1}{Q_2^{2/3}})} .$$

The ratios Q_n are given by (5a) and (5b).

Eq.(15) has been checked with the crosspower spectral density measurement and the agreement was within $\pm$ 20%. If the gain in channel n, V_n, is chosen so that $\frac{V_1}{V_2} = \frac{W_2}{W_1}$ uncorrelated signals produce circles, and we have the simple relation

$$\frac{a^2}{b^2} = 1 + Q_1^{2/3}(\omega) + Q_2^{2/3}(\omega) \quad . \tag{16}$$

CONCLUSIONS

Regarding the comparison of crosspower and autopower spectral density measurements it was found from the experimental investigations that two-detector crosscorrelation experiments give reliable results down to Q_{max}-values of about 0.1 whereas the limit for single-detector-autocorrelation experiments is about $Q_{max} = 2$, particularly if more than one break frequency exists in the transfer function. The maximum possible gain of 20 in detector efficiency applying the crosscorrelation technique is especially useful for experiments in fast systems. The increased analysing time for crosscorrelation measurements with small ratios Q can be reduced if a magnetic tape recorder and the tape speed-up technique is applied. Another reduction is due to the fact that the upper break frequency is large in fast systems (about 1 kcps) and so data analysis is not necessary down to 1 cps. In view of the difficulties to have highly efficient detectors in fast systems the conclusion is that two-detector crosscorrelation experiments should be conducted even if two separate channels are required.

Another advantage of the two-detector experiment is the capability for the study of space- and energy dependent effects in fast thermal coupled systems because crosscorrelation measurements between different zones of such systems should give more insight into the coupling mechanism than single-detector autocorrelation measurements at different positions. Although much work has still to be done in this respect, the two-detector experiment seems to be helpful for these investigations.

The optical demonstration of correlation, which works with two detecting channels only, may be helpful in setting up experiments. A quick check is possible to what extent correlated contributions are present in the signals.

REFERENCES

1 H.MEISTER, K.H.BECKURTS, W.HÄFELE, W.H.KÖHLER, K.OTT, The Fast-Thermal Argonaut Reactor, Concept, KFK-Report No.217 (1964).

2 D.STEGEMANN et al., The Fast Zero Energy Assembly SNEAK and its Experimental Program, Proceedings of the VIII Nuclear Congress, Rome, June 1963.

3 H.BORGWALDT and D.STEGEMANN, A Common Theory for Neutronic Noise Analysis Experiments in Nuclear Reactors, Nukleonik, 7, 313-325, (1965).

4 M.EDELMANN, G.KUSSMAUL, H.MEISTER, D.STEGEMANN, W.VÄTH, Pulsed Source and Noise Measurements on the STARK-Reactor, Proceedings of a IAEA-Symposium on Pulsed Neutron Research Karlsruhe, May 1965, Vol.II, 799 ff, (1965).

5 R.L.RANDALL and C.W.GRIFFIN, Application of Power Spectra to Reactor-System Analysis, Proceedings of the Symposium on Noise Analysis in Nuclear Systems, Gainesville, November 1963, AEC-Symposium, Series No.4.

6 J.S.BENDAT, Priciples and Applications of Random Noise Theory, 272 ff, John Wiley, New York, (1958).

7 W.VÄTH, Thesis (Diplom), Technical University Karlsruhe, (1966).

LIST OF FIGURES AND TABLES

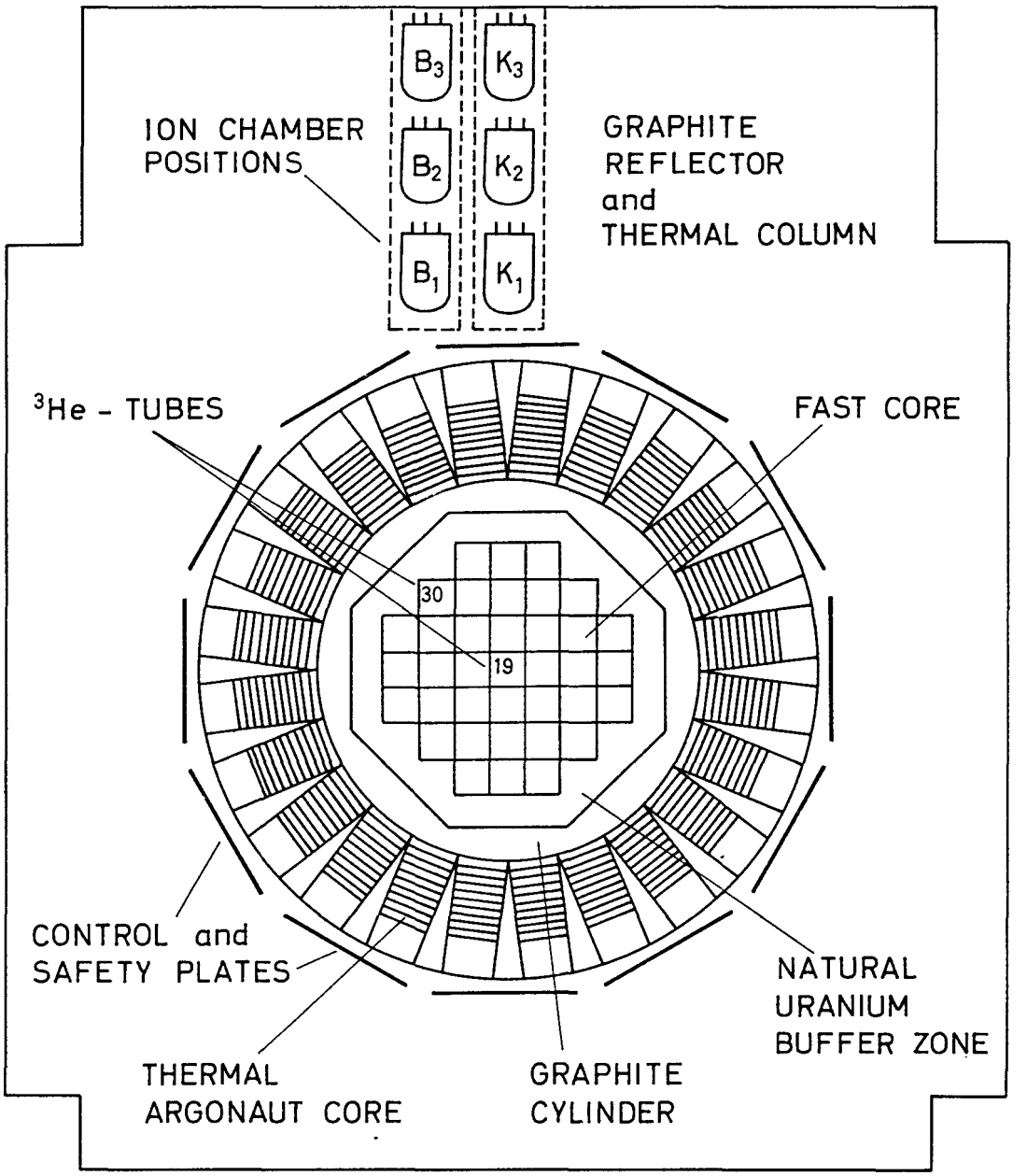

DETECTORS USED

1. Positions 19 and 30 : ^{3}He-filled counting tubes
   Type 339 S (pressure 10 atm ^{3}He, length 12", diameter 0.625")
   Texas Nuclear Corporation

2. Positions K_1-K_3 and B_1-B_3: ^{10}B-loaded, γ-compensated ion chamber
   Type RC 6
   20th Century Electronics

FIG. 1 SCHEMATIC CROSS SECTION OF STARK INCLUDING DETECTOR POSITIONS

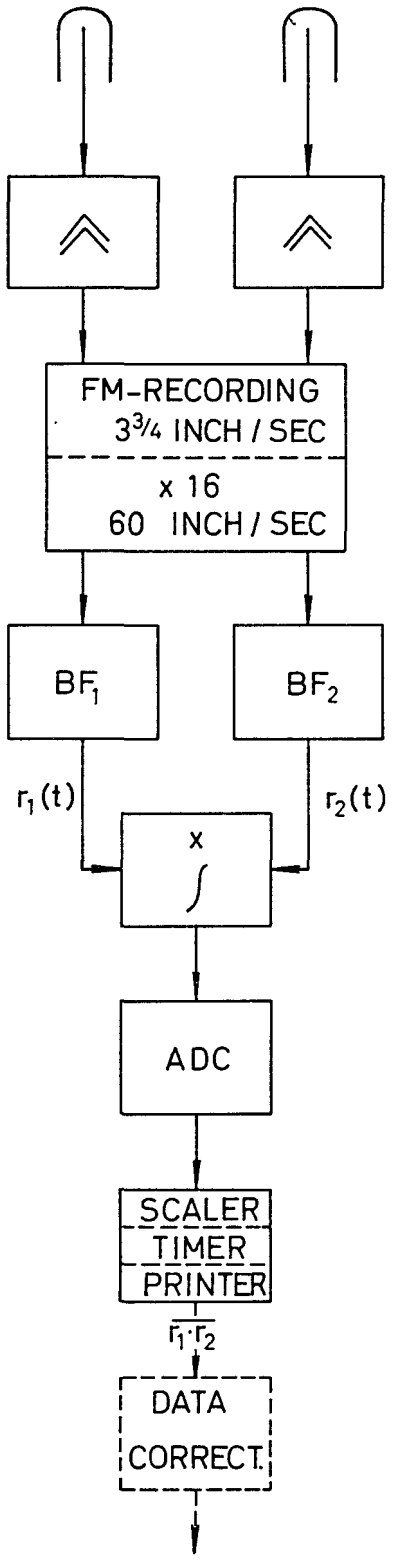

NEUTRON DETECTORS
RC 6 , TEXLIUM 339 S

AC - AMPLIFIERS
KEITHLEY 103

TAPE RECORDER
AMPEX FR 1300
PLAY BACK SPEED FACTOR

BAND PASS FILTERS
KROHN - HITE 330 M

MULTIPLIER and INTEGRATOR
PACE TR 10

ANALOG - TO - DIGITAL-CONVERTER
DYMEC 2210

NORMAL PULSE
COUNTING EQUIPMENT

CORRECTIONS FOR TAPE SPEED UP,
EQUIPMENT FREQUENCY RESPONSE
etc.

FIG. 2 DATA ACQUISITION AND REDUCTION SYSTEM FOR CROSS POWER SPECTRAL DENSITY MEASUREMENTS

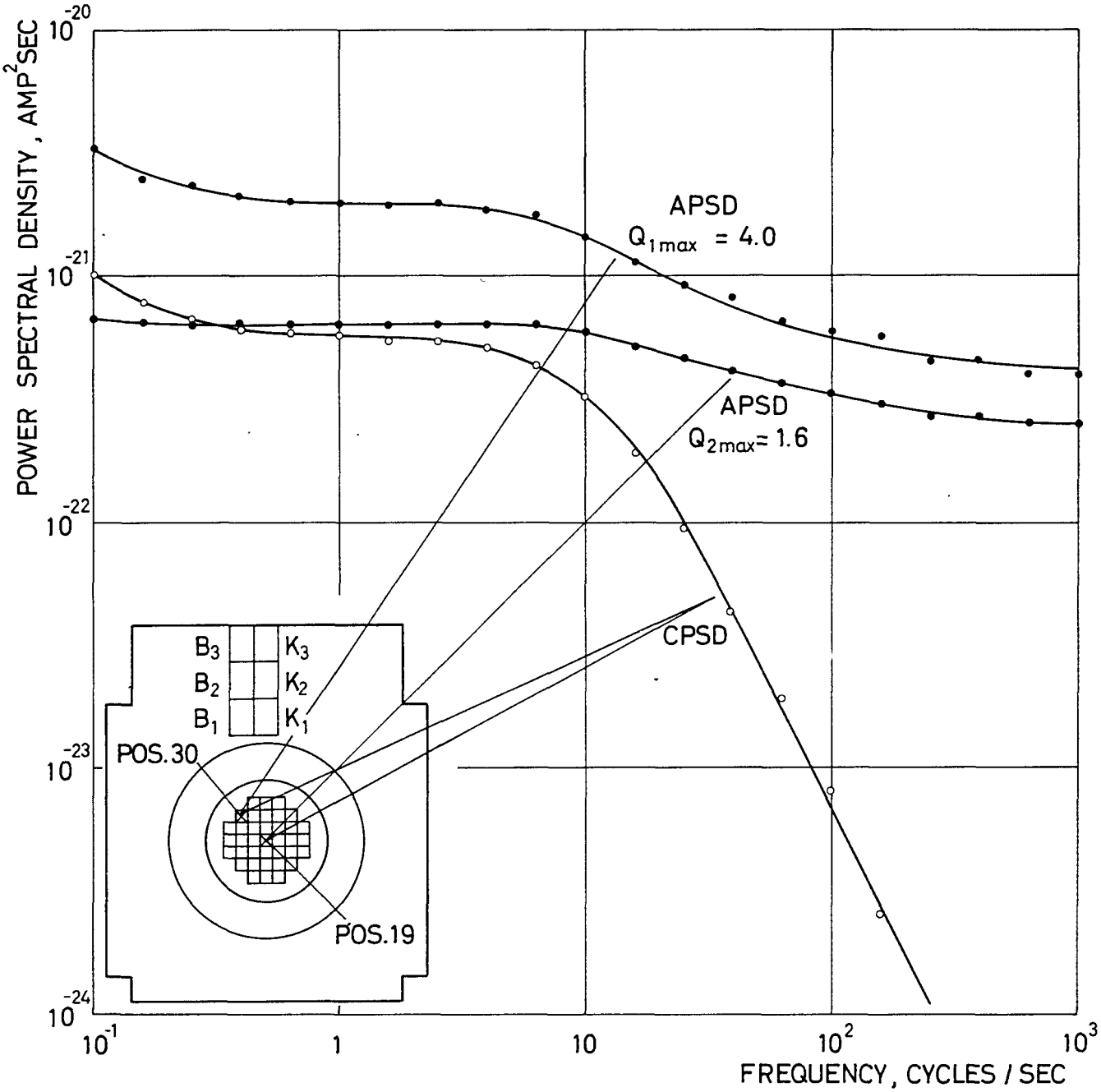

FIG. 3 AUTOPOWER SPECTRAL DENSITY (APSD) AND CROSS POWER SPECTRAL DENSITY (CPSD) VERSUS FREQUENCY IN THE FAST CORE. RUN NO 1-3

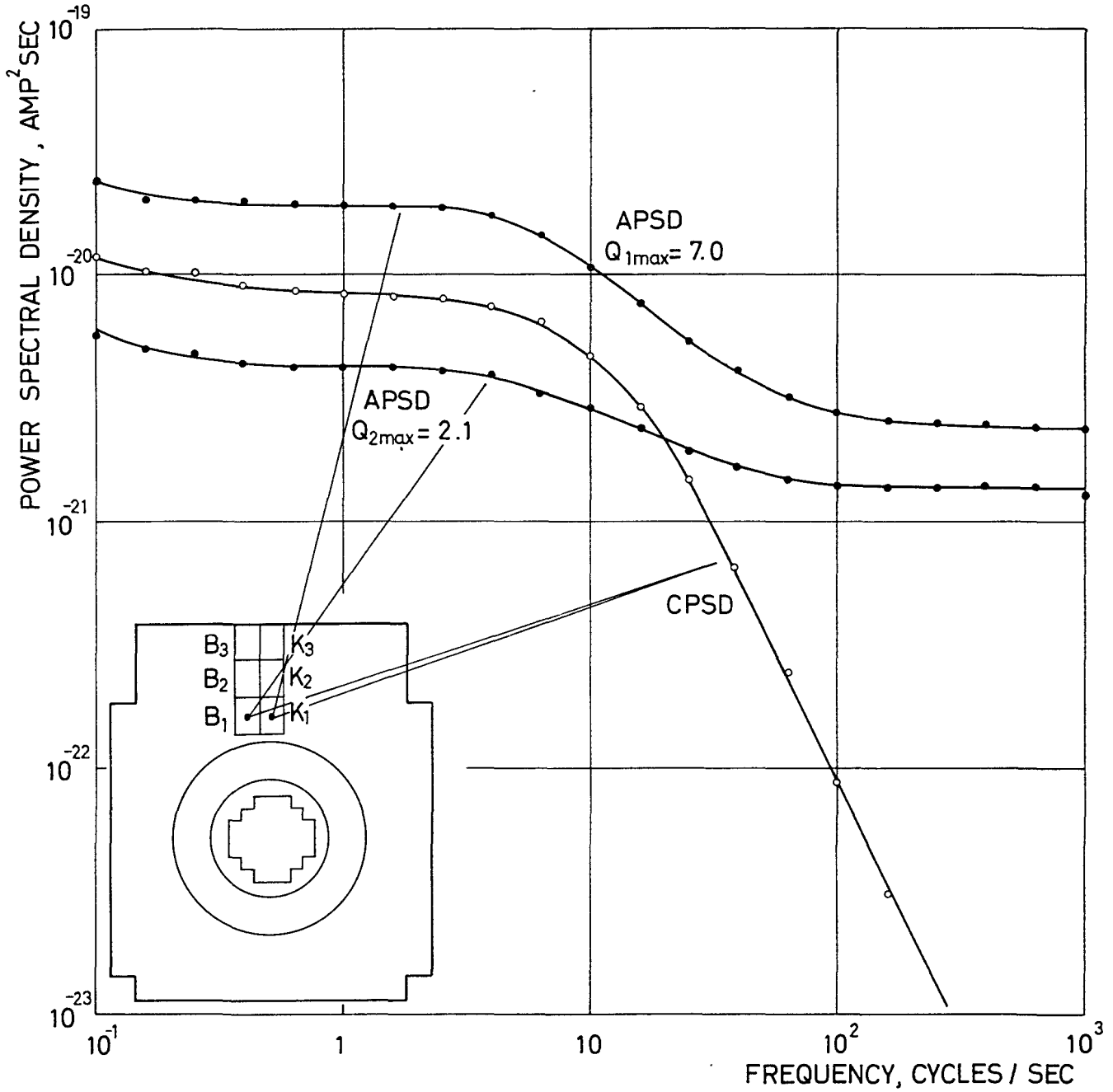

FIG. 4 AUTOPOWER AND CROSS POWER SPECTRAL DENSITY VERSUS FREQUENCY IN THE THERMAL ZONE. RUN NO 4-6

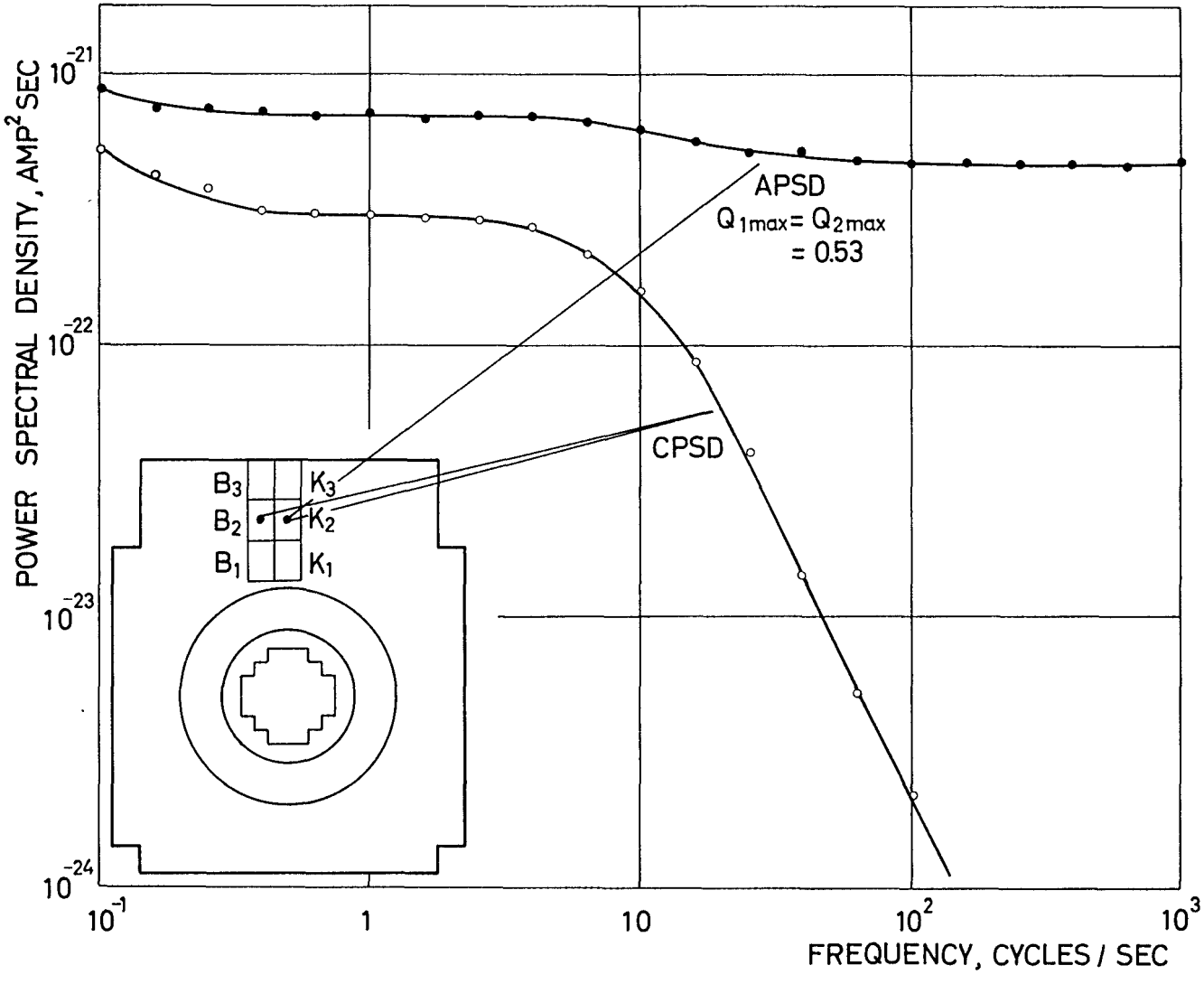

FIG. 5 AUTOPOWER AND CROSS POWER SPECTRAL DENSITY VERSUS FREQUENCY IN THE THERMAL ZONE. RUN NO 7 AND 8

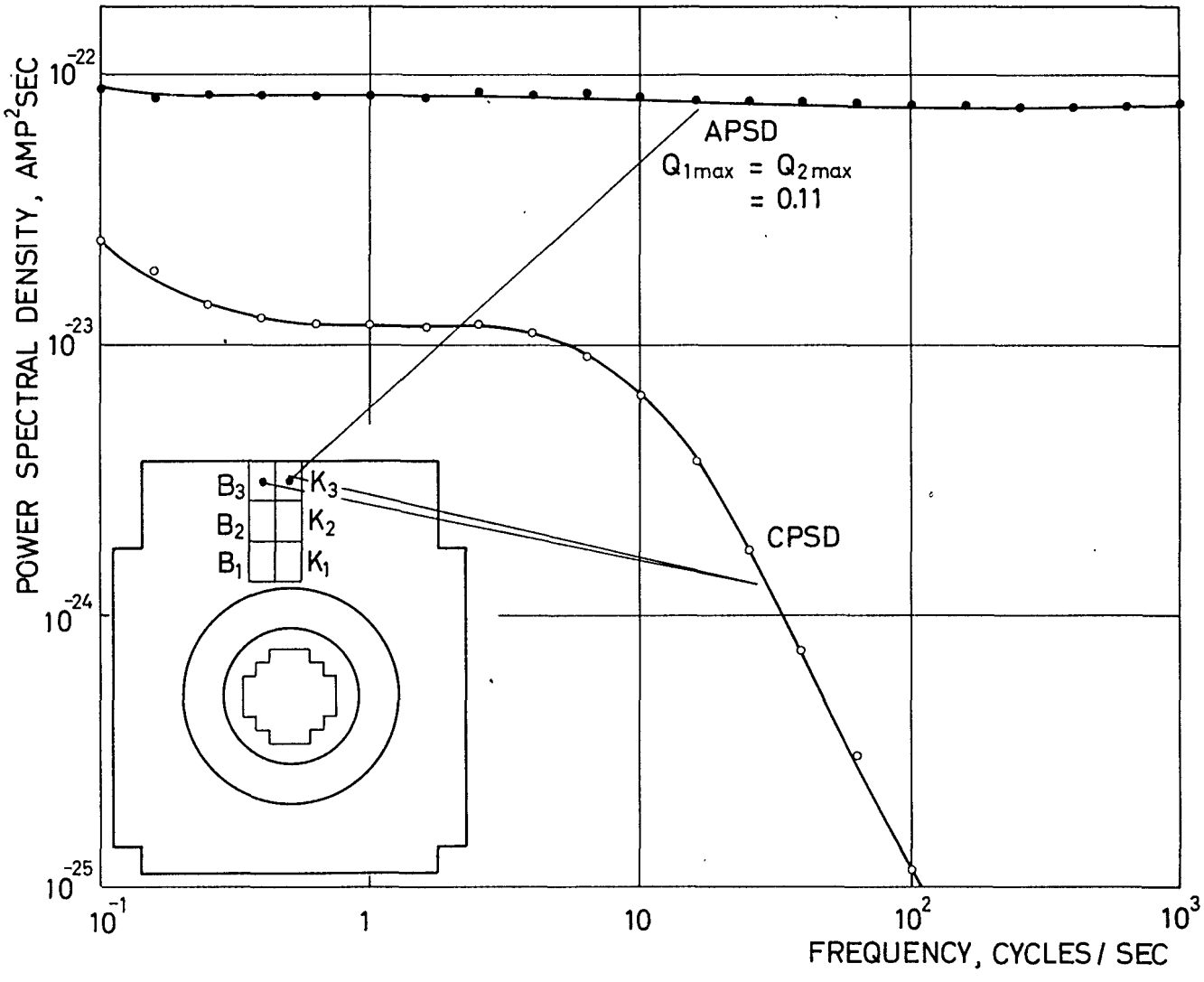

FIG. 6 AUTOPOWER AND CROSS POWER SPECTRAL DENSITY VERSUS FREQUENCY IN THE THERMAL ZONE. RUN NO 9 AND 10

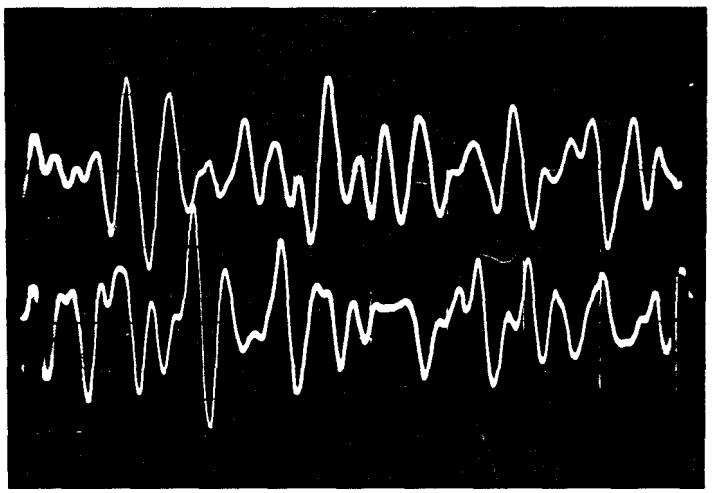

FIG. 7 UNCORRELATED FILTER OUTPUT SIGNALS IN A TWO DETECTOR CROSSCORRELATION EXPERIMENT

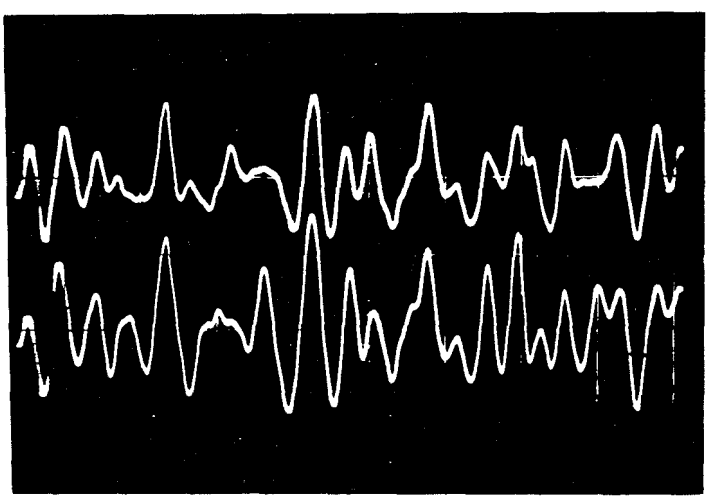

FIG. 8 PARTLY CORRELATED FILTER OUTPUT SIGNALS IN A TWO DETECTOR CROSSCORRELATION EXPERIMENT

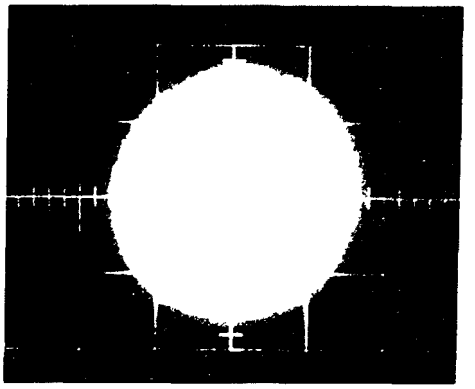

FIG. 9a UNCORRELATED SIGNALS

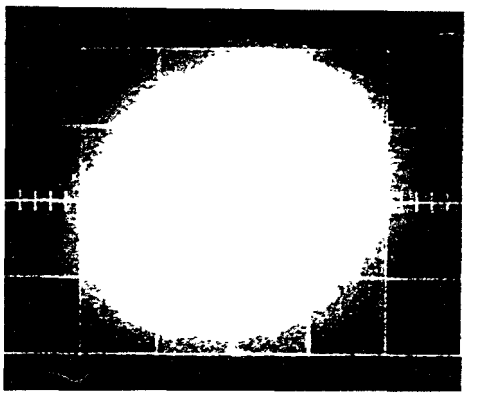

FIG. 9b PARTLY CORRELATED SIGNALS (F=40 CPS)

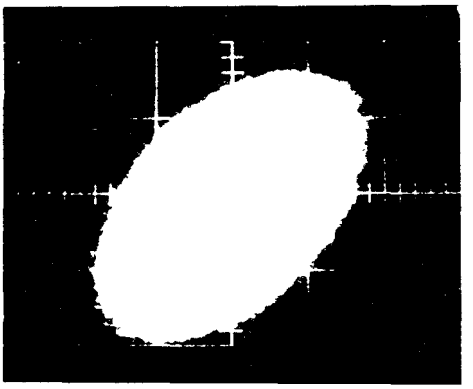

FIG. 9c PARTLY CORRELATED SIGNALS (F=15 CPS)

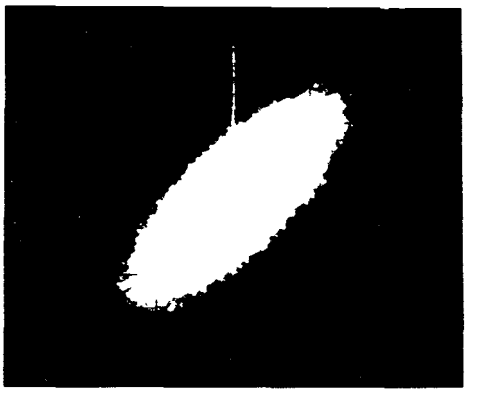

FIG. 9d PARTLY CORRELATED SIGNALS (F = 1 CPS)

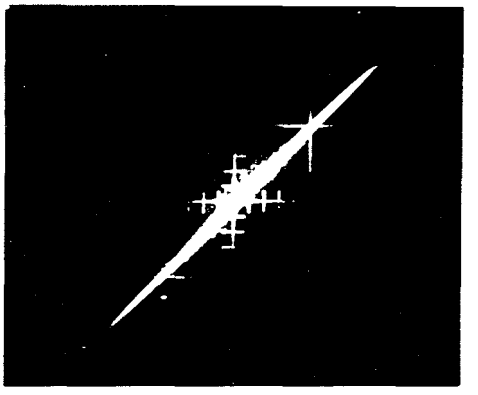

FIG. 9e AUTOCORRELATED SIGNALS

FIG. 9a - e OPTICAL DEMONSTRATION OF CORRELATION

RUN NO.	TYPE OF EXPERIMENT	FAST CORE POSITIONS	THERM.ZONE POSITIONS	RATIO $Q_{n\,max}$	DECAY CONST. $\alpha_c = \beta/\ell\,[sec^{-1}]$	RESULTS IN FIG.
1	AUTO	19	-	1.6	-	3
2	AUTO	30	-	4.0	66 $\pm$3	3
3	CROSS	19-30	-	'/.	65.9$\pm$2	3
4	AUTO	-	K_1	7.0	64.5$\pm$2.5	4
5	AUTO	-	B_1	2.1	67 $\pm$2	4
6	CROSS	-	K_1-B_1	'/.	67 $\pm$2	4
7	AUTO	-	$B_2 \approx K_2$	0.53	-	5
8	CROSS	-	K_2-B_2	'/.	64.5$\pm$2.5	5
9	AUTO	-	$B_3 \approx K_3$	0.11	-	6
10	CROSS	-	K_3-B_3	'/.	65.9$\pm$3	6

TAB.1 EXPERIMENTAL RUNS

RUN NO.	CENTER FREQUENCY f cps	$\pi \Delta f T$	$Q_{1\ max}$	$Q_{2\ max}$	Q_n n=1,2	ε_{CPSD}(Calc) in %	ε_{CPSD}(Exp) in %
a_1	1	30 566	7.0	2.1	-	0.93	1.4
a_2	1	30 566	0.53	0.53	-	1.8	2.1
a_3	1	30 566	0.11	0.11	-	5.8	3.5
b_1	1	17 182	-	-	0.53	2.3	2.3
b_2	2.5	42 595	-	-	0.50	1.4	1.9
b_3	6.3	24 054	-	-	0.38	2.4	1.7
b_4	10	38 182	-	-	0.27	2.5	1.6
b_5	25	45 456	-	-	0.076	4.8	3.8
b_6	63	240 549	-	-	0.014	15.5	22.6

TAB.2 COMPARISON OF THEORETICAL AND EXPERIMENTAL RELATIVE STANDARD DEVIATIONS FOR CROSSPOWER SPECTRAL DENSITY MEASUREMENTS